Supplementary information for

Structural basis for Ebola virus nucleocapsid assembly and function regulated by VP24

Yoko Fujita-Fujiharu[1,2,3,#,†], Shangfan Hu[1,2,3,#], Ai Hirabayashi[1,3], Yuki Takamatsu[4], Yen Ni Ng[1,2,3], Kazuya Houri[1,2,3], Yukiko Muramoto[1,2,3], Masahiro Nakano[1,2,3], Yukihiko Sugita[1,2,5], Takeshi Noda[1,2,3,6,*]

[1]Laboratory of Ultrastructural Virology, Institute for Life and Medical Sciences, Kyoto University, 53 Shogoin Kawahara-cho, Sakyo-ku, Kyoto 606-8507, Japan

[2]Laboratory of Ultrastructural Virology, Graduate School of Biostudies, Kyoto University, 53 Shogoin Kawahara-cho, Sakyo-ku, Kyoto 606-8507, Japan

[3]CREST, Japan Science and Technology Agency, 4-1-8 Honcho, Saitama, Kawaguchi 332-0012, Japan

[4]Department of Virology, Institute of Tropical Medicine, Nagasaki University, Sakamoto, Nagasaki City, Nagasaki 852-8102, Japan.

[5]Hakubi Center for Advanced Research, Kyoto University, Kyoto 606-8501, Japan

[6]Institute for Integrated Cell-Material Sciences, Kyoto University, Yoshida-Honmachi, Sakyoku, Kyoto 606-8501, Japan

[#]contributed equally

[*]corresponding author: noda.takeshi.6e@kyoto-u.ac.jp

[†]current address: Department of Cell and Virus Structure, Max Planck Institute of Biochemistry, Martinsried, Germany

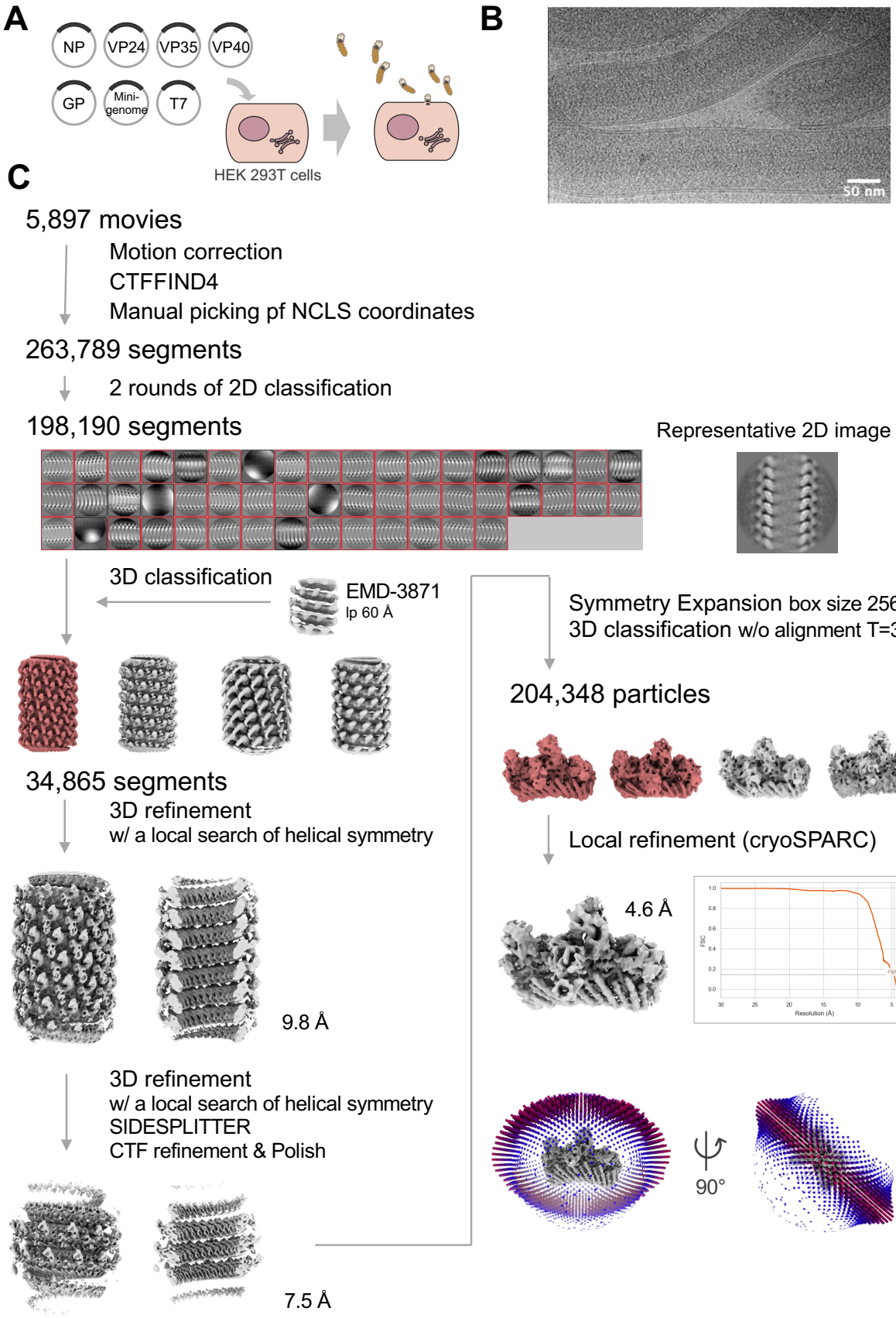
A
NP
VP24
VP35
VP40
GP
Mini-genome
T7
HEK 293T cells
B
50 nm
C
5,897 movies
Motion correction
CTFFIND4
Manual picking pf NCLS coordinates
263,789 segments
2 rounds of 2D classification
198,190 segments
Representative 2D image
3D classification
EMD-3871
lp 60 Å
34,865 segments
3D refinement
w/ a local search of helical symmetry
9.8 Å
3D refinement
w/ a local search of helical symmetry
SIDESPLITTER
CTF refinement & Polish
7.5 Å
Symmetry Expansion box size 256
3D classification w/o alignment T=32
204,348 particles
Local refinement (cryoSPARC)
4.6 Å
FSC
Resolution (Å)
90°

Supplementary Figure 1 Cryo-EM data processing of the NCLSs in VLPs.

A. Schematic representation of the VLPs production in HEK 293T cells.

B. Representative cryo-EM image of purified VLPs. Scale bar represents 50 nm.

C. Summary of the cryo-EM data processing workflow. The FSC curve and the angular distribution of the final reconstruction are shown at the right bottom. Most processes executed using RELION software, except for local refinement with cryoSPARC.

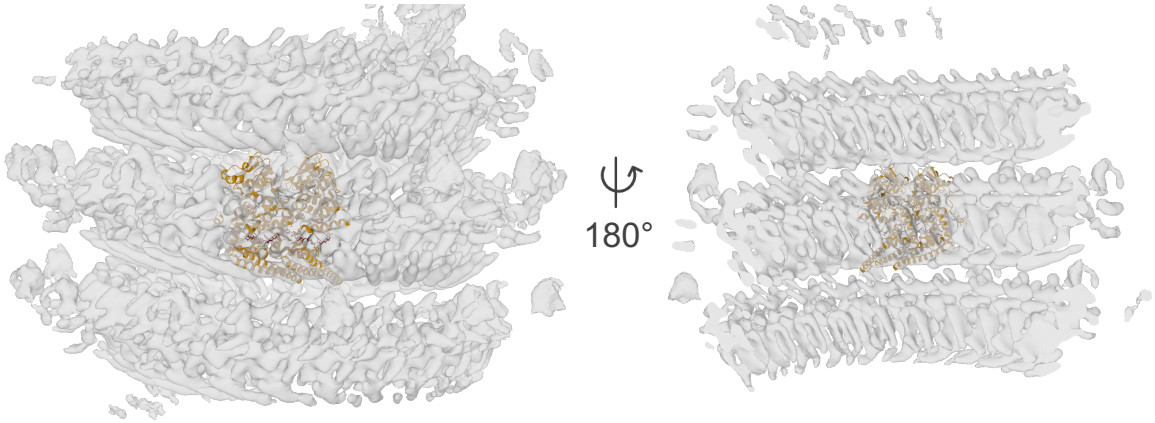

Supplementary Figure 2 Comparative visualization of the EBOV NCLS obtained via cryo-EM and the previously determined NP–RNA complex.

The cryo-EM map obtained in this study using helical symmetry (shown in gray) is superimposed on the atomic model of the purified NP–RNA complex structure[22] (PDB ID: 5Z9W) shown in orange. Density thresholds were set to indicate the inner helical densities.

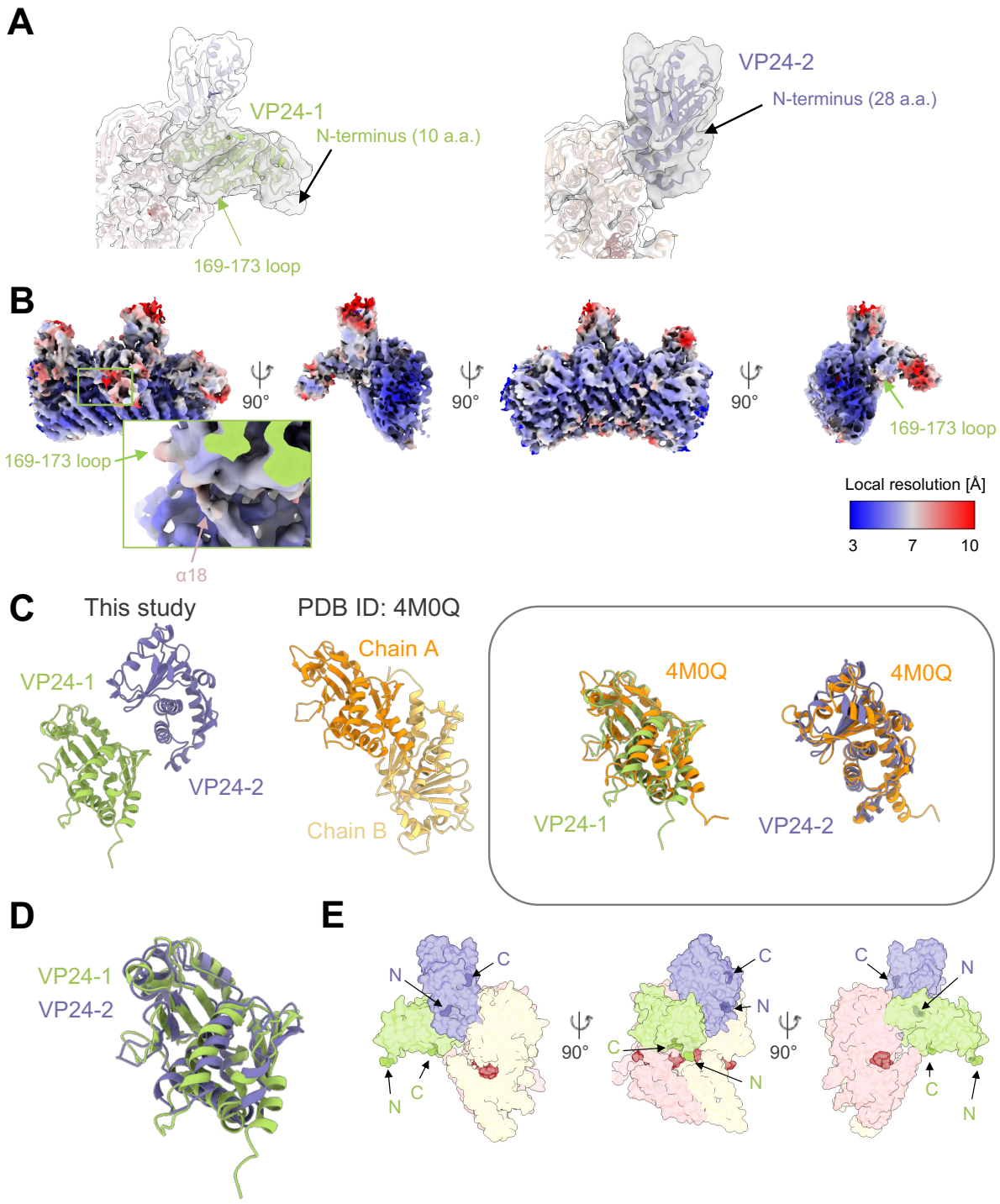

Supplementary Figure 3 Detailed structural comparison of VP24 interaction interfaces, comparing them with previously reported structures

A. Close-up views of VP24-1 (10 a.a. to 231 a.a.) and VP24-2 (28 a.a. to 231 a.a.), with cryo-EM map (shown in gray). A black arrow indicates each N-terminus, and a light green arrow indicates the 169-173 loop.

B. Local resolution map of the helical repeating unit. A light green arrow indicates the 169-173 loops. The surface is colored according to the local resolution as defined by the color map to the right.

C. Comparison of our VP24-1 and VP24-2 models from this study with the crystal structure of EBOV VP24 in the dimer form[26] (PDB ID: 4M0Q). The right panel shows the structural comparisons of our VP24 models from the PDB 4M0Q chain A.

D. Structural comparison of VP24-1 and VP24-2 from this study.

E. Surface representation with highlighted N- and C-termini of VP24s.

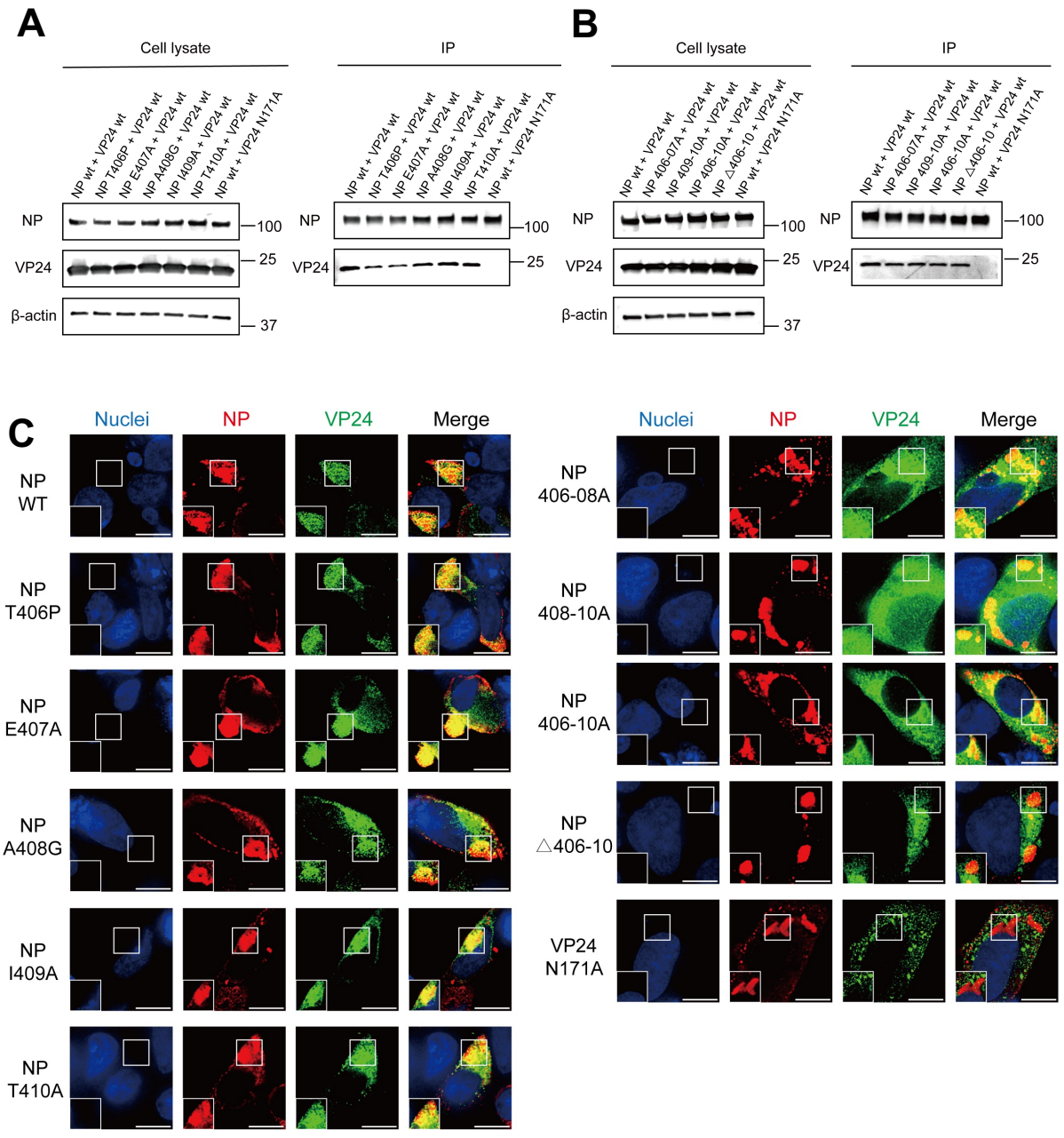

Supplementary Figure 4 Mutational analysis of NP at helix α18.

A, B. Immunoprecipitation assay using either FLAG-tagged NP with a single mutation (A) or FLAG-tagged NP with multiple mutations (B) as well as VP24. Left panel, whole cell lysates of cells transfected with FLAG-tagged NP mutant and VP24 were analyzed using western blotting using anti-VP24 and anti-NP antibodies. Beta-actin was detected as a loading control. Right panel, VP24 co-immunoprecipitated with FLAG-tagged NPs using an anti-FLAG antibody were analyzed using western blotting using anti-VP24 and anti-NP antibodies. Experiments were performed three times independently. Source data are provided as a Source Data file.

C. Localization of NP mutants and VP24 in cells co-expressing FLAG-tagged NP mutants, VP24, and VP35.The cells were immunostained using anti-FLAG (red) and anti-VP24 (green) antibodies. Nuclei were stained with Hoechst 33342 (blue). Experiments were performed three times independently. Source data are provided as a Source Data file. Scale bars represent 10 μm. NP, nucleoprotein; IP, immunoprecipitation

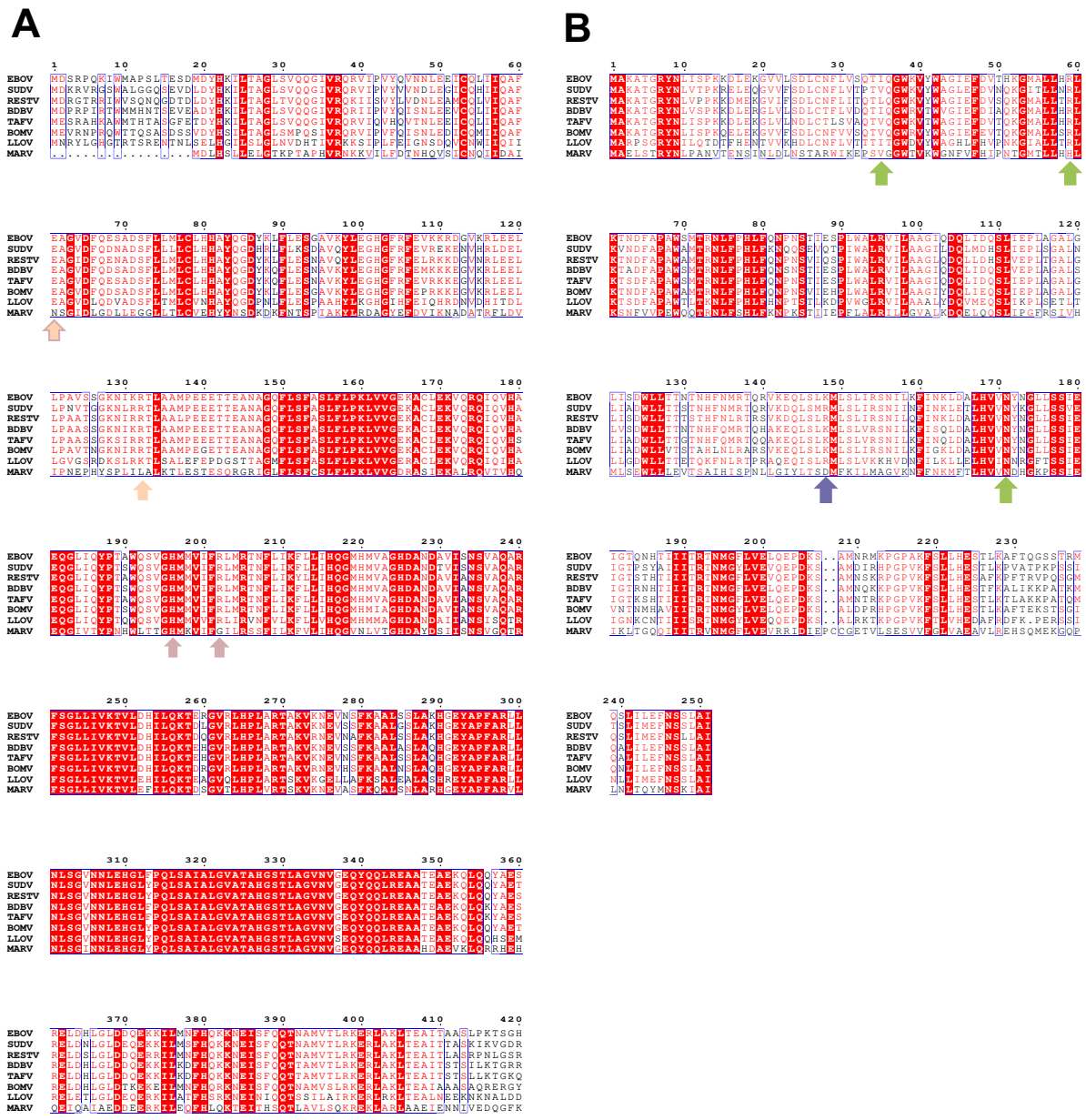

Supplementary Figure 5 Sequence alignment of the NP and VP24 among filoviruses

The amino acid sequences of filovirus (A) NP and (B) VP24 (EBOV: *Zaire ebolavirus* {NCBI accession number: P18272 and Q05322}, SUDV: *Sudan ebolavirus* {NCBI accession number: Q9QP77 and Q5XX02}, RESTV: *Reston ebolavirus* {NCBI accession number: Q8JPY1 and Q77DB4}, BDBV: *Bundibugyo ebolavirus* {NCBI accession number: B8XCM7 and B8XCN4}, TAFV: *Taï Forest ebolavirus* {NCBI accession number: B8XCN6 and B8XCP3}, BOMV: *Bombali ebolavirus* {NCBI accession number: A0A4D5SFX8 and A0A343EQF5}, LLOV: *Lloviu cuevavirus* {NCBI accession number: G8EFI1 and G8EFI8}, MARV: *Marburg marburgvirus* {NCBI accession number: Q1PD53

and Q1PD62}) were aligned with ClustalW2.1[1] and visualized using ESPript 3.0[2]. The number of alignments was assigned based on EBOV sequences. Conserved residues are highlighted in red, similar residues are colored in red, and both residues are outlined in blue. The amino acids mentioned in the manuscript are indicated by arrows in the same color, as shown in Figure 1.

Supplementary Table 1. Comparison of helical parameters in EBOV NC-related structures

	This study	EMD-6903	EMD-3871	EMD-3873
Target	VLP	NP–RNA complex	VLP	Infectious virion
Method	Single-particle analysis	Single-particle analysis	cryo-ET	cryo-ET
Pitch	75.55 Å	73.56 Å	75 ± 3 Å	74 ± 1 Å
Number of unit per turn	12.8	24.4 for 1-mer NP means 12.2 for 2-mer NPs	12.8 or 13.8	11.9 or 12.9

Supplementary Table 2. Cryo-EM data collection, refinement and validation statistics

	EBOV NCLS in VLPs (EMDB-39081) (PDB ID 8Y9J)
Data collection and processing	
Voltage (kV)	300
Electron exposure (e–/Å^2)	60
Defocus range (μm)	-0.625 to -2
Pixel size (Å)	0.88
Initial particle images (no.)	263,789
Final particle images for the helical reconstruction (no.)	34,865
Final particle images for the symmetry expanded particles (no.)	204,384
Map resolution for the symmetry expanded particles (Å)	4.6
FSC threshold	0.143
Refinement	
Initial model used (PDB code)	5Z9W, 4M0Q, 6EHM
Model resolution (Å)	4.5
FSC threshold	0.143
Model resolution range (Å)	4.3-7.0

Map *B* factor	173.9
Model composition	
Non-hydrogen atoms	9773
Protein residues	1205
Nucleotide	12
B factors (Å^2)	
Protein	263.63
Nucleotide	225.73
R.m.s. deviations	
Bond lengths (Å)	0.012
Bond angles (°)	2.100
Validation	
MolProbity score	1.78
Clashscore	2.14
Poor rotamers (%)	2.23
Ramachandran plot	
Favored (%)	90.64
Allowed (%)	7.35
Disallowed (%)	2.01

Supplementary References

1. Larkin, M. A. *et al.* Clustal W and Clustal X version 2.0. *Bioinforma. Oxf. Engl.* **23**, 2947–2948 (2007).
2. Robert, X. & Gouet, P. Deciphering key features in protein structures with the new ENDscript server. *Nucleic Acids Res.* **42**, W320–W324 (2014).